Tanzania Journal of Engineering and Technology 2024, **43**(2):75 - 90
OPEN ACCESS articles distributed under Creative Commons
Attribution Licence [CC BY-ND]
Websites: https://ajol.org/tjet; https://tjet.udsm.ac.tz



ISSN 1821-536X (**print**); ISSN 2619-8789 (**electronic**)
https://doi.org/10.52339/tjet.v43i2.908

*Regular Research Manuscript*

# Development and Testing of Small-Scale Flash Dryer for Maize Bran

**Eden Ngowi[1†], Justin M. Jeremiah[1], Lilian Kaale[2] and Emrod Elisante[1]**

[1]Department of Chemical and Process Engineering, College of Engineering and Technology, University of Dar es Salaam, P.O. Box 35131, Dar es Salaam, Tanzania
[2]Department of Food Science and Technology, College of Agriculture and Food Technology, University of Dar es Salaam, P. O. Box 35134, Dar es Salaam, Tanzania
[†]Correspondence Author: edengowi@gmail.com
[†]ORCID: https://orcid.org/0009-0009-0090-8389

## ABSTRACT

*Sun drying is the most common technique used to dry various food products due to its economic convenience. However, it is not effective owing to its unreliable nature leading to microbial deterioration and aflatoxin contamination of food. In Tanzania, about 1.3 million tonnes of maize bran are at risk of deterioration annually due to improper drying. The aim of this study was to design, fabricate and test an efficient small-scale flash dryer for maize bran. Using principles of material and energy balance, a small-scale flash dryer with a throughput of 500 kg of dry product per hour was designed resulting in a nominal diameter of 387 mm and a drying length of 20 m. Design calculations and drawings were done using MS Excel 2021 and SolidWorks 2018 respectively. Empirical procedures were used to fabricate and test the dryer. The material of construction used in the flash duct was food grade (stainless steel, SS 201). A fuel blend of Waste Engine Oil (WEO) and diesel (85%-15%) was used with a novel heavy oil burner. It was observed that at an inlet air temperature of 150 °C and air velocity of 12 m/s, moist maize bran was dried from 37% to 10% w.b. The fabricated flash dryer's energy efficiency, specific energy consumption, and specific energy utilization are 74%, 3.4 MJ/kg water evaporated, and 1.71 MJ/kg dry maize bran respectively. It was concluded that the fabricated small-scale flash dryer displayed improved energy performance compared to others presented in literature. Better instrumentation was recommended for feedback control on burner operation and process monitoring which further enhances the performance of the fabricated small-scale flash dryer.*

ARTICLE INFO
Submitted: May **31, 2023**
Revised: Apr**. 27, 2024**
Accepted: **June. 15, 2024**
Published: **Aug., 2024**

**Keywords:** *Small-scale Flash Dryer, Maize Bran, Specific Energy Consumption, Energy Efficiency.*

## INTRODUCTION

Food security is amongst the prevailing challenges in Sub-Saharan Africa (SSA) and maize has proven its ability to curb the predicament having an annual per-capita consumption ranging from 94 to 100 kg (Udomkun et al., 2017). In local maize flour mills, the main by-product is maize bran which has become the main ingredient in animal feeds. During the maize dehulling process, maize bran is produced in a moist state. This poses a risk since high moisture content above 13% in food and high ambient temperatures common in SSA create a conducive environment for microbial infestations especially the Aspergillus fungi which are known to produce aflatoxins, a fatal type of mycotoxin (Achaglinkame et al., 2017). Exposure to aflatoxins triggers adverse health conditions in both animals and humans, culminating to death in severe cases (Kumar et al., 2017). Also, huge economic losses may be incurred as the market value of aflatoxin-contaminated food decreases (Kaale et al., 2021).

From time immemorial, sun and solar drying have been employed as the most cost-effective techniques to extend the shelf-life of food and feed like maize bran (Chiewchan et al., 2015). Despite their affordability, there is low quality consistence due to its inherent dependence on fluctuating weather conditions which calls for longer drying times, and they require large floor areas for processing (Romuli et al., 2017). Other drying technologies such as tray drying can only handle low throughputs and have long batch times which fail to match with the high maize bran production rates in most local maize mills (Mujumdar, 2015).

The use of flash dryers, also known as Pneumatic Conveyor Dryers (PCDs), is highly recommended for free-flowing particulate materials like maize bran since intimate contacting of the particles and gas phase occurs, bringing about fast drying rates and thus high processing capacities (Hecht et al., 2019). Medium to large-scale flash drying plants are capital intensive, costing up to US$68,500 per plant, which makes them impossible to own by small and medium scale entrepreneurs (SMEs) (Adegbite et al., 2023). This implies that small-scale flash dryers are of practical importance to SMEs.

Despite the suitability of small-scale flash dryers for maize bran, they are still faced with low energy performance (Precoppe et al., 2016). This is evident in most flash dryers used to dry cassava products in Nigeria which have average energy efficiencies below 30% and high specific energy consumption in the range of 4 to 6 MJ/kg water evaporated (Ojide et al., 2022). This low energy performance is largely attributed to poor design and improper operation of these dryers (Tran et al., 2022). Therefore, the objectives of this study were: (i) To design, fabricate and test an efficient small-scale flash dryer for processing particulate feeds (up to 3 mm) such as maize bran; and (ii) To establish the energy performance of the fabricated small-scale flash dryer.

### Theoretical Principles

Drying involves the removal of small amounts of moisture from solids by thermal means. Some motivations for drying include: (i) preservation to prolong a product's shelf life; and (ii) property modification of particulate materials such as flowability, compressibility, weight and volume, making them easier to handle, store and transport (Xiao & Mujumdar, 2020).

In flash dryers, drying is achieved by contacting wet solids with hot air in a concurrent fashion in a flow duct. This facilitates rapid heat and mass transfer between the solid and gas phases thus fast drying rates can be achieved (Banooni et al., 2018). Due to their high effectiveness, flash dryers have very high throughputs, reaching up to 400 tonnes per day, for large-scale units (Chapuis et al., 2017). The basic components of flash dryers include: (i) Flash Duct; (ii) Air Heater; (iii) Cyclone Separator; (iv) Blower; and (v) Feeder System (Satpati et al., 2020). Material and Energy Balance is the prime step in sizing a flash dryer. To simplify engineering design calculations, all processes are assumed to occur at steady-state (Adegbite et al., 2023).

## MATERIAL AND ENERGY BALANCE

The solids and air streams pass through the flash dryer as depicted in **Figure 1**. The balances are performed specifically about the boundaries of the flash duct.

### *Mass Balance about the Flash Dryer*

During drying, there is moisture transfer from the solid phase to the air phase. Thus, only moisture balance is performed across the flash dryer as follows:

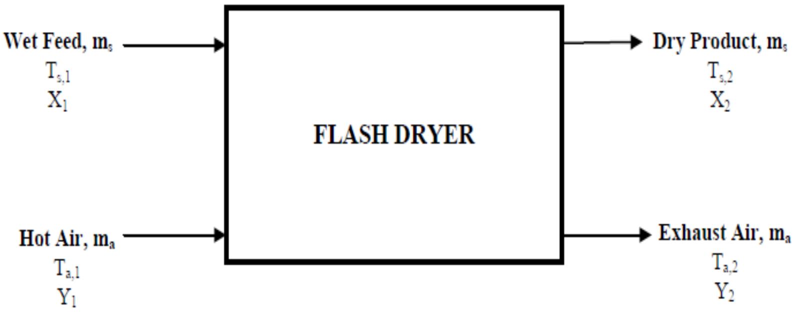


**Figure 1: Material and energy flow across the flash duct.**

$$m_aY_1 + m_SX_1 = m_aY_2 + m_SX_2$$
$$m_a(Y_2 - Y_1) = m_S(X_1 - X_2) \quad (1)$$

### Energy Balance about the Flash Dryer

A thermal energy balance about the flash dryer accounts for all stream enthalpies with the associated heat losses to the environment as in (2), while the wet solids enthalpy change and moist air enthalpy change are given by Equations 3 and 4 respectively

$$m_ah_{a,1} + m_sh_{s,1} = m_ah_{a,2} + m_sh_{s,2} + Q_{losses}$$
$$m_a(h_{a,1} - h_{a,2}) = m_s(h_{s,2} - h_{s,1}) + Q_{losses} \quad (2)$$

$$h_{s,2} - h_{s,1} = Cp_{ds}(T_{s,2} - T_{s,1}) + Cp_w[X_2(T_{s,2} - T_{ref}) - X_1(T_{s,1} - T_{ref})] \quad (3)$$

$$h_{a,1} - h_{a,2} = Cp_{da}(T_{a,1} - T_{a,2}) + [\,Cp_v(T_{a,1} - T_{ref}) + \lambda_{ref}]Y_1 - [Cp_v(T_{a,2} - T_{ref}) + \lambda_{ref}]Y_2 \quad (4)$$

Upon substitution of Equations 3 and 4 into Equation 2 and solving the resulting equation simultaneously with Equation 1 gives the values of the required air mass flowrate $m_a$ (and therefore the air volumetric flowrate, $\dot{V}_a$) and air exhaust humidity, $Y_2$.

### Flow Velocities

#### Air Velocity

The air velocity should be high enough to transport the largest solid particle in the flash duct (Kuye *et al*., 2017). For a system consisting of *both* horizontal and vertical sections, the *saltation velocity* is the *minimum* design air velocity**.** The design air velocity is generally set to be 50% greater than the saltation velocity (Klinzing, 2018)**.** Equation 5 gives an accurate value of saltation velocity over wide range of conditions (Gomes & Mesquita, 2014).

$$u_{SALT} = \left[\frac{4\dot{m}_s 10^d g^{\frac{x}{2}} D^{\left(\frac{x}{2}-2\right)}}{\rho\pi}\right]^{\frac{1}{x+1}} \quad (5)$$

where: $d = 1.44d_p + 1.96$ (in $mm$); and $x = 1.10d_p + 2.5$ (in $mm$)

#### Particle Velocity

It follows that the *slip velocity* is approximately equal to the particle's terminal velocity at hydrodynamic steady-state (Gomes & Mesquita, 2014). Equations 6 and 7 give the design particle velocity.

$$u_R = u_a - u_s \approx u_t \quad (6)$$

$$Re_t = (2.33Ar^{0.018} - 1.53Ar^{-0.016})^{13.3} \quad (7)$$

### Dimensions of the Flash Duct

The continuity equation is used together with Equation 5 to obtain both the *nominal diameter* of the flash dryer and air velocity. Once the particle velocity and residence time are known, the design *length* of the drying duct is obtained using Equation 8.

$$L = \tau u_s \tag{8}$$

### Particle Drying Time

For a spherical wet particle of instantaneous radius $R$ and dry crust radius $R_o$, the particle drying time ($t$) is the *minimum* residence time ($\tau_{min}$) the particle should spend in the dryer as obtained by Equations 9 through 14 (Nugraha *et al.*, 2022).

$$\tau \geq t = \frac{\rho_w}{\left(\rho_{v,o} - \rho_{v,\infty}\right)} \left[\frac{(R - R_o)}{h_m} + \frac{{R_o}^2}{6\mathcal{D}_{va}}\right] \tag{9}$$

where:

$$\frac{P\mathcal{D}_{AB}}{\left(P_{cr,A}P_{cr,B}\right)^{\frac{1}{3}}\left(T_{cr,A}T_{cr,B}\right)^{\frac{5}{12}}(1/M_A + 1/M_B)^{\frac{1}{2}}} = a\left(\frac{T}{\sqrt{T_{cr,v}T_{cr,a}}}\right)^b \tag{10}$$

(*For water – air mixture:* $a = 3.64 \times 10^{-4}$ and $b = 2.334$).

$$h_{\text{m}} = \frac{\mathcal{D}}{d_p} Sh \tag{11}$$

$$Sh = \frac{ln(1 + B_M)}{B_M} Sh_0 \tag{12}$$

$$B_M = \frac{Y_{v,s} - Y_{v,\infty}}{1 - Y_{v,s}} \tag{13}$$

$$Sh_0 = 2 + 0.69Re^{\frac{1}{2}}Sc^{\frac{1}{3}} \tag{14}$$

### Pressure Drop Along the Flash Dryer

Energy losses in flash dryers occur along three main components: (i) Air heater; (ii) Flash duct; and (iii) Cyclone**.**

### Pressure Drop Along the Air Heater

Equation 15 gives the pressure drop along the air heater (Incropera *et al.*, 2017).

$$\Delta P_{AH} = N_L f_x \left(\frac{\rho u_{max}^2}{2}\right) \tag{15}$$

### Pressure Drop Along the Flash Duct

This is mainly due to acceleration of the gas-solid flow ($\Delta P_{acc}$); gravity ($\Delta P_g$); and wall friction losses ($\Delta P_f$) given by Equations 16 through 19 (El-Behery *et al.*, 2017).

$$\Delta P_{duct} = \Delta P_{acc} + \Delta P_g + \Delta P_f \tag{16}$$

where:

$$\Delta P_{acc} = \varepsilon[0.5\rho {u_a}^2] + (1 - \varepsilon)[0.5\rho_s {u_s}^2] \tag{17}$$

$$\Delta P_g = \varepsilon[\rho g H] + (1 - \varepsilon)[\rho_s g H] \tag{18}$$

$$\Delta P_f = \varepsilon\left[f_D \frac{L}{D}\frac{\rho {u_a}^2}{2}\right] + (1 - \varepsilon)\left[f_S \frac{L}{D}\frac{\rho_s {u_s}^2}{2}\right] \tag{19}$$

For smooth pipes, the fluid-wall and particle-wall friction factors are given by Equations 20 and 21 respectively (Munson *et al.*, 2018).

$$f_D = 0.314Re^{-0.25} \quad (20)$$

$$f_p = 1.0503{Fr_p}^{-1.831} \quad (21)$$

### Pressure Drop Across the Cyclone

Several phenomena account for the pressure drop across the cyclone such as: (i) Inlet Contraction; (ii) Particle Acceleration; (iii) Barrel Friction; (iv) Gas Flow Reversal; and (v) Exit Contraction (Knowlton & Shrinkant, 2019).

### Blower Sizing

The blower power requirement is given by Equations 22 and 23 (Munson *et al.*, 2018).

$$N = \frac{\dot{V}_a \Delta P_T}{\eta} \quad (22)$$

where:

$$\Delta P_T = \Delta P_{AH} + \Delta P_{duct} + \Delta P_{cyclone} \quad (23)$$

### Dryer Performance Indicators

For any dryer, three main measures have been established to gauge their energy performance, namely: (i) Specific Energy Consumption, $q_s$: the energy consumed per unit water evaporated; (ii) Specific Heat Utilization, $q_u$ : the energy consumed per unit of dry product and (iii) Energy Efficiency, $\eta_E$ : energy required for moisture vaporisation per total energy consumed (Kemp, 2012).

## MATERIALS AND METHODS

### Design, Fabrication and Testing of Small-Scale Flash Dryers

*Approach on Design of the Small-Scale Flash Dryer*

No standards exist for the design of flash dryers. Thus, a design procedure was devised where Material and Energy Balance (MEB) was first done about the flash dryer to obtain the required air mass flowrate ($\dot{m}_a$) and exhaust air humidity ($Y_2$) as shown in **Figure 2**. MS Excel 2021 was used to perform the design calculations using the design equations presented in theory. Computer Aided Drafting (CAD) software such as AutoCAD 2020 and SolidWorks 2018 were used to document the dryer's design drawings.

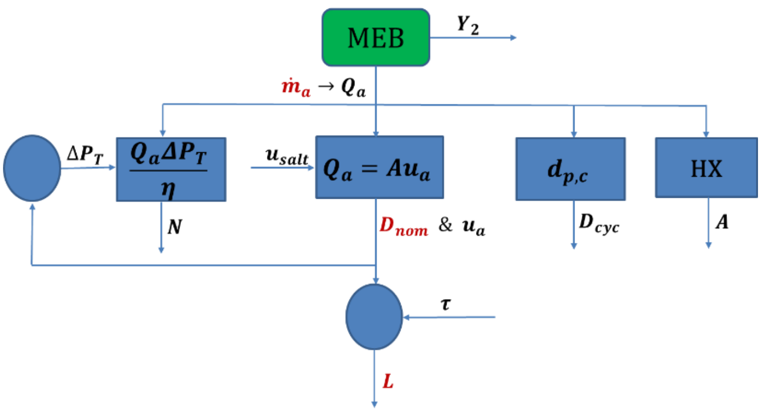


**Figure 2: Design path used in this study.**

*Approach on Fabrication of the Small-Scale Flash Dryer*

The materials of construction used were *stainless-steel* (SS 201) for components coming in contact with maize bran such as the flash duct and cyclone separator; and *mild steel* (MS) for the rest of the parts. No standards for fabrication of flash dryers exist thus an empirical procedure (with its accompanying tools and methods) was devised as follows:

i. All flash dryer components were cut

from SS and MS sheets according to the design drawings using angle grinders and CNC plasma cutters

ii. All cut parts pertaining to the flash duct were rolled into ducts using a roller machine.

iii. Preliminary setting and assembly of parts were done by spot welding (Tungsten Inert Gas (TIG) welding for SS sheets and stick welding for MS sheets).

iv. Full welding was done after final confirmation of preliminary assembly settings.

v. The support structure for the flash duct was fabricated and erected on proposed site.

vi. The flash dryer sub-systems were assembled at flange points with gaskets to prevent leakage using a chain block and other pulley-based lifting mechanisms.

vii. Approach on Testing of the Small-Scale Flash Dryer

viii. No any national or international standards are in place for the testing of flash dryers. Thus, the testing of the fabricated dryer was done according to the following procedure:

ix. Initial fuel level (h_o) was recorded and the burner was switched on for 20 min to warm up the heat exchanger. A known mass of wet maize bran (m_wb) was also put into the feeder hopper.

x. The blower was then switched on and left to run for 10 min for the dryer to reach steady-state where the target inlet air temperature was 150 °C.

xi. The screw feeder and disperser were also switched on 3 min before the release of wet maize bran into the flash duct in so that the motors would not start with load which could have caused damaging high starting currents.

xii. Wet maize bran was then released into the throat of the flash duct's venturi section by opening the feeder hopper's bottom outlet. The stop watch is started at this moment. Also. The current fuel level (h_1) was recorded.

xiii. On completion of drying process, the burner was switched off and the stop-watch was paused, marking the end of the drying test. The mass of dried maize bran (m_db) is also measured and recorded using weigh scale.

xiv. The final fuel level (h_2) was then recorded while the blower was left online to cool the dryer to near-ambient temperature as displayed on the temperature indicator and controller.

xv. The blower was switched off after cooling the dryer.

The dryer tests were done for 5 days. After every 10 minutes of steady-state operation, samples for wet and dry maize bran were collected in properly sealed glass jars which were temporarily stored in a cool box and later taken to the analytical laboratory of the Department of Chemical and Process Engineering of the University of Dar es Salaam for moisture content determination (105 °C for 2 hours in a convection oven according to TZS 34-1). MS Excel 2021 was used to perform all statistical analyses. Instruments and methods used for data collection are as shown in Table I.

**Table I: Instruments and Methods of Data Collection**

| Data | Instruments/Methods |
|---|---|
| Air humidity | Capacitive hygrometer, model 5359202 and relative humidity meter, BTH model BHC31 |
| Air velocity | Digital vane anemometer, MASTECH model MS6252A |
| Air temperature | Thermocouples, type K and manual temperature-data module, AUTONICS model TCN4S-24R, accuracy: ± 2 °C |
| Surface temperature | Hand-held infrared thermometer, BENETECH GM320 |
| Solid moisture content | Oven drying at CPE Department, UDSM (WTB Binder, Model Number 990419) |

| | |
|---|---|
| Mass flowrates | Weigh scale, AVERY, Type 307, Model B4657-306 and Stopwatch |
| Fuel consumption | Level meter |

**Establishment of Energy Performance of the Fabricated Flash Dryer**

The water evaporation rate, fuel consumption, specific energy consumption, specific energy utilization and energy efficiency were computed in this work by Equations 24 through 28.

Water Evaporation Rate:
$$\dot{m}_w = \frac{m_{wb} - m_{db}}{t} \quad (24)$$

Fuel Consumption:
$$V_{fuel} = A(h_2 - h_1) \quad (25)$$

Specific Energy Consumption:
$$q_s = \frac{C.V \times V_{fuel}}{m_w} \quad (26)$$

Specific Energy Utilization:
$$q_u = \frac{C.V \times V_{fuel}}{m_{dp}} \quad (27)$$

Energy Efficiency:
$$\eta_E = \frac{m_w \lambda}{C.V \times V_{fuel}} \quad (28)$$

## RESULTS AND DISCUSSIONS

### Design and Fabrication of the Small-Scale Flash Dryer

To match the typical throughput (up to 40 tonnes of maize per day) of the most local maize millers in Tanzania, the flash dryer was designed to process *500 kg of dry solids per hour*. Other design specifications are summarised in Figure 3.

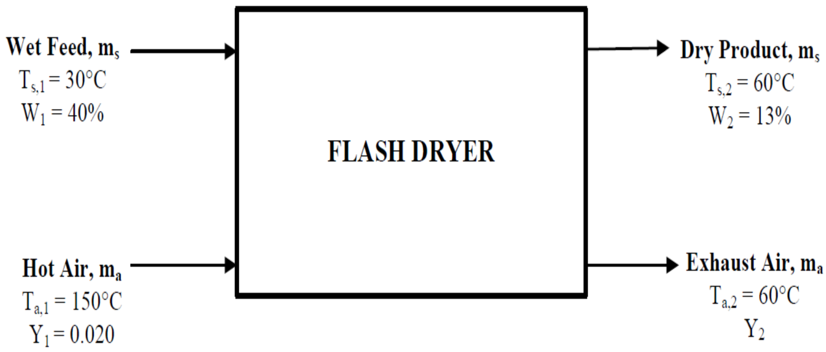


**Figure 3: Design data for the small-scale flash dryer.**

High inlet air temperature in the range of 120 to 180 °C is acceptable since solid particles in the flash dryer experience short residence times in the order of 2 seconds reducing the probability of nutrient denaturation in food (Chapuis *et al*., 2017). A thermal equilibrium at 60 °C was assumed for dry product and exhaust air (Precoppe *et al*., 2016). To accommodate a wide range of materials, the feed moisture content was set at 40% w.b while the target dry product moisture content was set at 13% w.b which guarantees reduced microbial activity (Achaglinkame *et al*., 2017).

Considering 20% heat losses to the environment, the required dry air mass flow rate was 7,250 kg/h with an exhaust air humidity of 56 g/kg dry air. Taking inlet hot air density into account, the design *maximum* air volumetric flow rate was 2.41 $m^3/s$. Other calculated design parameters are summarised in Table II. The resulting design geometry of the flash dryer is shown in *Figure 4* displaying the simple-to-construct and assemble camel-back geometry with two expansion zones which help reduce the local flow velocities which in turn increase the particle residence time in the flash duct.

**Table II: Other Design Parameters of the Fabricated Flash Dryer**

| Design Parameters | Design Values |
|---|---|
| Flow Velocity: Solid, $u_s$; Air, $u_a$ | 16.87 m/s; 20.54 m/s |
| Residence Time, $\tau$ | 1.2 s |
| Heat Exchanger Area, $A_{HX}$ | 12 $m^2$ |
| Cyclone Body Diameter, $D_{cyc}$ | 700 mm |
| Flash Dryer Pressure Drop, $\Delta P_T$ | 5034 Pa |
| Blower at 80% Efficiency, $\eta$ | 11 kW |

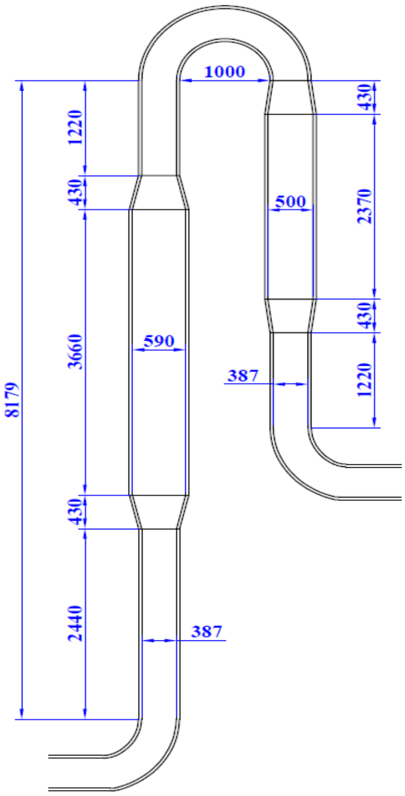


**Figure 4: Geometry of designed flash duct**

The fabricated flash dryer has the highest design capacity with the longest drying duct with a wider nominal diameter as shown in Table III.

A tube-bank heat exchanger with the highest heat transfer area was used uniquely in this work. Also, a negative pressure system was used in the fabricated flash dryer similar to the work by Precoppe *et al.*, 2016 and Adegbite *et al.*, 2023 to reduce the blower power requirement.

Based on the design results, the flash dryer assembly model is as shown in Figure 5. Ambient air (in blue arrows) enters underneath the air heater for heating while wet solids enter by the feeder. They then travel concurrently (in black arrows) through the flash duct where drying takes place. Air-solid separation occurs in the cyclone where dried solids exit the dryer (in orange arrows) and exhaust air is vented out through the blower. Temperature readings during drying operation is recorded from thermocouples installed along the flash dryer as indicated by TC-0 to TC-8 while HX-I and HX-O represent Heat Exchanger In and Out; VI and VO: Venturi In and Out; and CYCL-I and CYCL-O represent the Cyclone In and Out.

**Table III: Comparison of different designs of small-scale flash dryers**

| Parameters | This Work | Kuye *et al.*, 2011 | Precoppe *et al.*, 2016 | Tran *et al.*, 2022 | Adegbite *et al.*, 2023 |
|---|---|---|---|---|---|
| **Design Capacity** | 822 kg wet feed per hour | 820 kg wet feed per hour | 180 kg wet feed per hour | 100 kg wet feed per hour | 300 kg wet feed per hour |

| | | | | | |
|---|---|---|---|---|---|
| **Drying Length** | 20 m | 6.12 m | 15 m | 24.84 m | 22.5 m |
| **Nominal Diameter** | 387 mm | 508 mm | 380 mm | 180 mm | 250 mm |
| **Burner Type** | Waste engine oil (WEO) | Diesel burner, WEO | Diesel burner, WEO | Diesel burner, WEO | Diesel burner, WEO |
| **Heat Exchanger** | Tube Bank, 12 $m^2$ | Double Pipe, 6 $m^2$ | Double Pipe, 6 $m^2$ | Shell and Tube, 7 $m^2$ | Shell and Tube, 7 $m^2$ |
| **Pressure System** | Negative | Positive | Negative | Positive | Negative |
| **Fan Power** | 15 hp | 3.5 hp | 10 hp | 10 hp | 15 hp |
| **Feed** | Screw, Impeller disperser, Horizontal Venturi | Screw, Cage mill disperser, Horizontal Venturi | Cage mill disperser, Vertical venturi | Screw, Cage mill disperser, Horizontal Venturi | Screw, Cage mill disperser, Horizontal Venturi |
| **Discharge** | Rotary Airlock | Dust trap with flap valve | Dust trap with flap valve | - | - |

Based on the design results, the flash dryer assembly model is as shown in Figure 5. Ambient air (in blue arrows) enters underneath the air heater for heating while wet solids enter by the feeder. They then travel concurrently (in black arrows) through the flash duct where drying takes place. Air-solid separation occurs in the cyclone where dried solids exit the dryer (in orange arrows) and exhaust air is vented out through the blower. Temperature readings during drying operation is recorded from thermocouples installed along the flash dryer as indicated by TC-0 to TC-8 while HX-I and HX-O represent Heat Exchanger In and Out; VI and VO: Venturi In and Out; and CYCL-I and CYCL-O represent the Cyclone In and Out.

### Operating Parameters of Flash Dryers

The fabricated flash dryer had the largest feeding rate with the lowest feed moisture content as shown in Table IV. Lowest values of the dry product moisture content were also observed in this work. All dryers depict air velocities within the same range. An 85%-15% WEO - diesel fuel blend was used in this work with high throughput while other works used fuel blends richer in diesel (> 20%) with lower throughputs, showing improved fuel economy

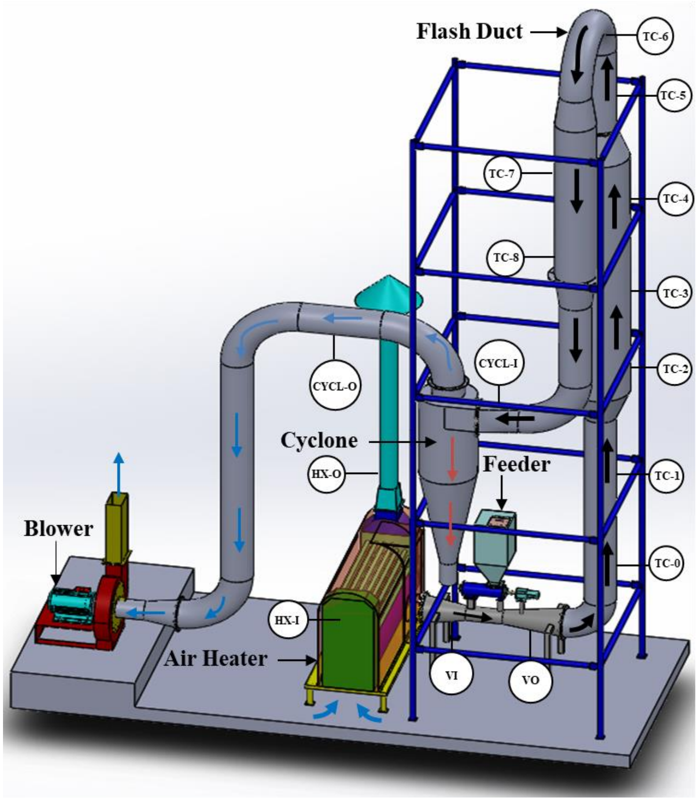


**Figure 5: Design model of the fabricated flash dryer.**

**Table IV: Comparison of operating parameters across different small-scale flash dryers**

| Operation Parameters | Units | Mean Values | | | |
|---|---|---|---|---|---|
| | | This Work | Precoppe *et al.*, 2017 | Tran *et al.*, 2022 | Adegbite *et al.*, 2023 |
| Wet Feed Mass Flowrate | kg/h | 822 ± 12.32 | 325.9 ± 45.7 | 98.6 | 298 ± 30.2 |
| Moisture Content of Wet Feed | % w.b | 37± 2.7 | 46.1 ± 0.8 | 43 ± 6 | 47.06 ± 5.2 |
| Dry Product Mass Flowrate | kg/h | 547 ± 15.62 | 208.05 ± 37 | 65 ± 5.5 | 186.34 ± 7.4 |
| Moisture Content of Dry Product | % w.b | 10 ± 1 | 15.3 ± 3.7 | 12 ± 6 | 9.60 ± 3.4 |
| Water Evaporation Rate | kg/h | 275 ± 9.32 | - | 33.6 ± 5.6 | 105.38 ± 2.7 |
| Air Mass Flowrate | kg/h | 6909 ± 352 | 2302.8 ± 6.4 | - | 4147.2 ± 9.8 |
| Air Velocity | m/s | 12 ± 0.62 | 10.2 ± 0.3 | - | 13 ± 1.2 |
| Heat Exchanger Exhaust Temperature | °C | 207 ± 1.27 | - | - | 215 ± 8.7 |
| Inlet Air Temperature | °C | 151 ± 0.80 | 275.6 ± 16.2 | 238.4 ± 9.5 | 180 ± 4.3 |
| Cyclone Inlet Air Temperature | °C | 72 ± 0.85 | - | - | 78 ± 1.8 |
| Blower Exhaust Air Temperature | °C | 62 ± 0.77 | 59.5 ± 1.4 | 60.7 ± 3.5 | 65.89 ± 4.9 |

| | | | | | |
|---|---|---|---|---|---|
| Blower Exhaust Air Relative Humidity | % | 43 ± 0.86 | 49.6 ± 5.6 | 55.3 ± 9.2 | 42.8 ±7.9 |
| Fuel Consumption | L/h | [1]27 ± 1.99 | [2]25.3 ± 2.5 | - | [2]9.2 ± 4.2 |

[1, 2] represents fuel consumption in L/h and kg/h respectively.

**Temperature Profiles Along the Flash Duct**

In this work, spatial and temporal temperature data were collected along the flash duct to monitor the fabricated flash dryer's temperature dynamics. However, there is limited temperature profile data in literature since flow geometries of flash ducts vary greatly. The flash dryer was pre-heated for 20 minutes as shown in *Figure 6*. At steady-state, the thermocouple for inlet air temperature (VI) registered 150 °C; cyclone inlet air (CYCL – I), 75 °C; and cyclone outlet air (CYCL – O), 65 °C. Other mid-way thermocouples (TC – 0, TC – 2, TC – 4) registered 115 °C, 110 °C and 90 °C respectively. After the drying test, the burner was switched off and cooling started from the 55$^{th}$ minute.

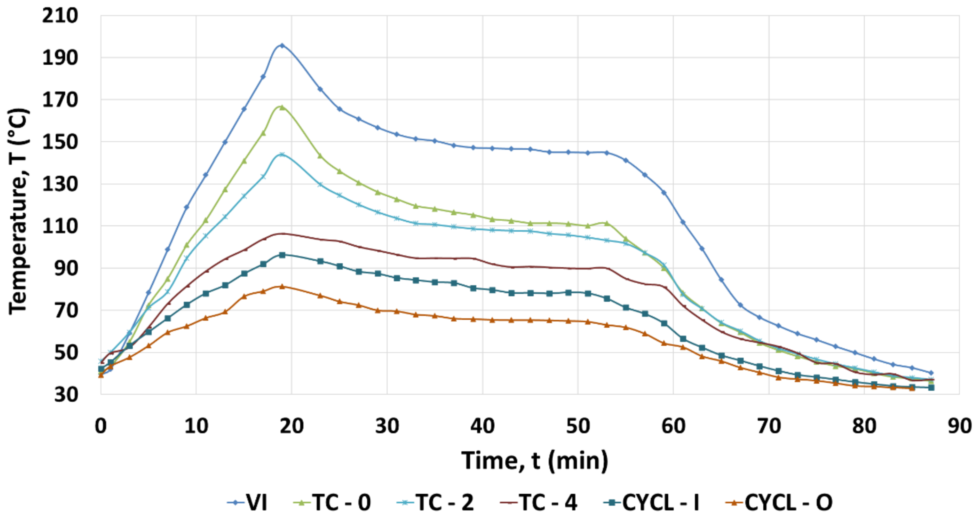


**Figure 6: Temperature-time profiles along the flash duct.**

Along the flash duct (3 - 12 m), there was a decrease in temperature to a minimum of 65 °C at the crest of the duct (13 m) as shown in *Figure 7*. This is because the air's enthalpy was progressively being used up to dry the cool wet solids as they travelled along the flash duct. However, an abrupt drop in temperature (2 m from the start of the flash duct) was due to the deceleration of hot air as it exited the venturi-throat causing inadequate mixing of adjacent air flow streams. A subsequent rise in temperature was also observed because of local hot air accumulation caused by an elbow which marked the start of the flash duct's ascending leg. Moreover, higher temperatures were observed at high velocities since heat extraction from the air heater was faster.

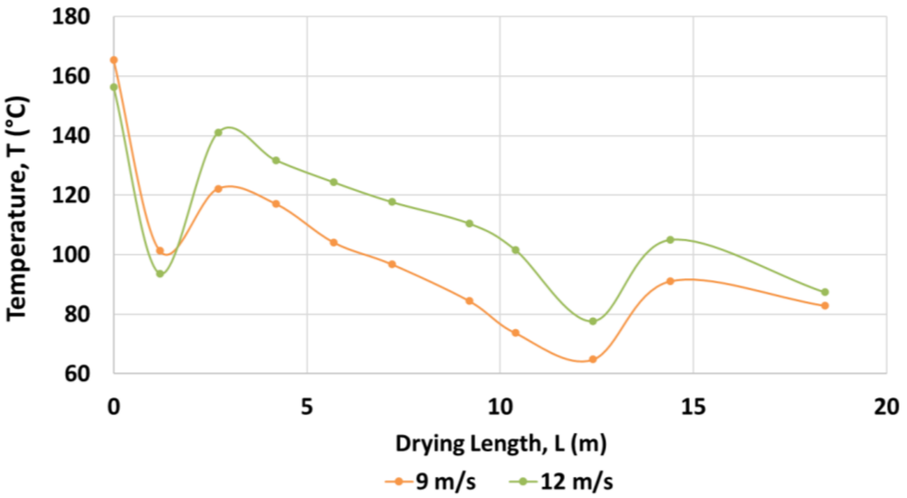


**Figure 7: Steady-State temperature profile along the flash duct.**

**Energy Performance Indicators of Small-Scale Flash Dryers**

The energy efficiency of convective dryers ranges from 20% to 60% (Banooni *et al.*, 2018). From **Figure 8**, the fabricated small-scale flash dryer has an average energy efficiency of 74% which is second highest showing improved energy performance.

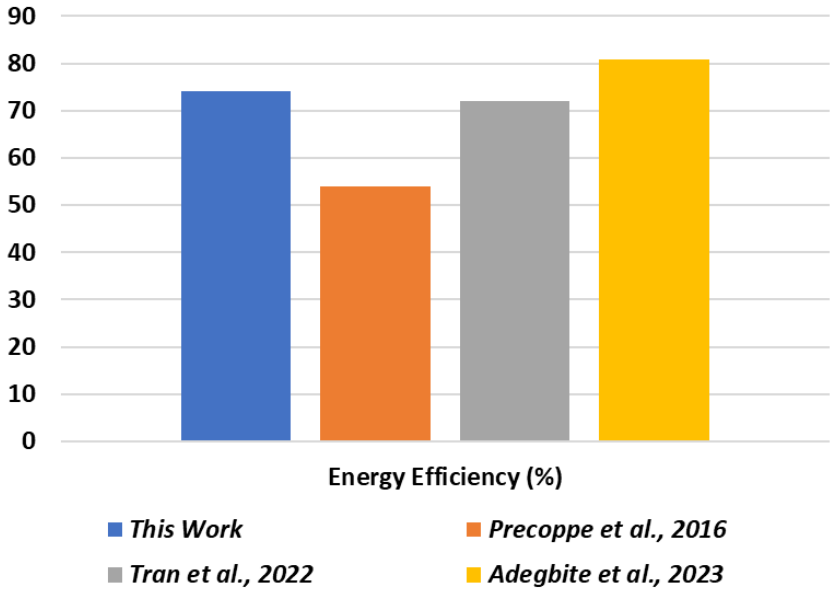


**Figure 8: Energy efficiencies across various small scale flash dryers.**

The ideal specific energy consumption of dryers is 2.5 MJ/kg water evaporated (Hecht *et al.*, 2019). However, this cannot be attained due to heat losses and sensible heat gained by solid particles during drying (Precoppe *et al.*, 2017). Most flash dryers are reported to have specific energy consumptions ranging from 4.5 - 9 MJ/kg water (Mujumdar, 2015). From **Figure 9**, the specific energy consumption and specific heat utilization of the fabricated small-scale flash dryer are 3.40 MJ/kg water evaporated and 1.71 MJ/kg dry maize bran respectively which are the lowest values thus showing improved energy performance.

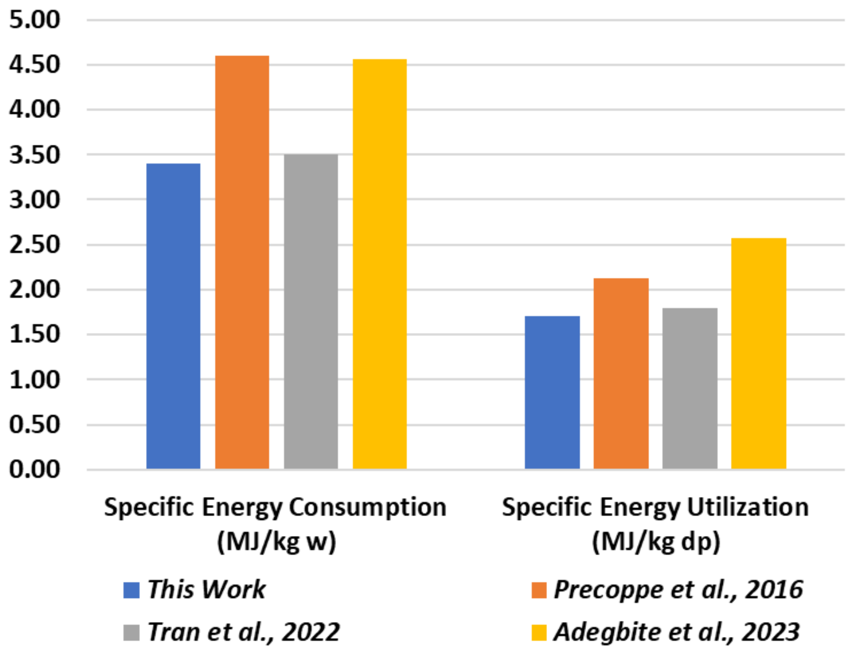


**Figure 9: Specific energy consumption and specific energy utilization across various small scale flash dryers.**

## CONCLUSION AND RECOMMENDATIONS

This study designed, fabricated and tested an improved small-scale flash dryer at an installed capacity of 822 kg of wet feed per hour with a drying length of 20 m and a nominal diameter of 387 mm. The fabricated small-scale flash dryer reduces the moisture content of wet maize bran from 37% to 10% w.b using inlet hot air at 150 °C. Moreover, it displays improved energy performance with an average specific energy consumption of 3.40 MJ per kg water evaporated; an average specific heat utilization of 1.71 MJ/kg dry maize bran; and an average energy efficiency of 74%. These performance indicators satisfy the need of small-scale maize processors and other food products such as cassava and wheat. This study recommends better instrumentation especially on the feedback control of the burner operation and data acquisition tools for better process monitoring.

## ACKNOWLEDGEMENT

Special thanks to INTEX for sponsoring the fabrication of the small-scale flash dryer prototype and technical support.

**Nomenclature**

| | |
|---|---|
| $A$ | Surface area [m$^2$] |
| $Ar$ | Archimedes number [-] |
| $B_M$ | Mass transfer Spalding number [-] |
| $CNC$ | Computer Numerical Control |
| $D$ | Diameter of the pipe [m] |
| $\mathcal{D}$ | Mass diffusivity [m$^2$/s] |
| $d$ | Particle size [m] |
| $d.b$ | Dry Basis |
| $f$ | Friction factor [-] |
| $f_x$ | Heat Exchanger Correction Factor [-] |
| $Fr$ | Froude number [-] |
| $g$ | Acceleration due to gravity [m/s$^2$] |
| $h$ | Specific enthalpy [J/kg] |
| $H$ | Maximum vertical height [m] |
| $h_m$ | Mass transfer coefficient [m/s] |
| $HX$ | Heat Exchanger |
| $L$ | Drying length [m] |
| $M$ | Molar mass [kg/kmol] |
| $\dot{m}$ | Mass flow rate [kg/s] |
| $N_L$ | Number of tubes [-] |
| $P$ | Pressure [Pa] |
| $Q$ | Thermal energy [J] |

| | |
|---|---|
| $q$ | Thermal power [W] |
| $R$ | Particle radius [m] |
| $Re$ | Reynolds number [-] |
| $Sc$ | Schmidt number [-] |
| $Sh$ | Sherwood number [-] |
| $T$ | Temperature [K] |
| $t$ | Time [s] |
| $u$ | Velocity [m/s] |
| $V$ | Vertical length [m] |
| $\dot{V}$ | Volumetric flowrate [$m^3/s$] |
| $W$ | Moisture content, wet basis [kg water/kg wet solid] |
| $w.b$ | Wet Basis |
| $X$ | Moisture content, dry basis [kg water/ kg dry solid] |
| $Y$ | Absolute humidity [kg vapour/ kg dry air] |

**Greek Alphabets**

| | |
|---|---|
| $\varepsilon$ | Voidage [-] |
| $\eta$ | Efficiency [%] |
| $\lambda$ | Latent heat of vapourisation [J/kg] |
| $\mu$ | Viscosity [Pa.s] |
| $\rho$ | Density [$kg/m^3$] |
| $\tau$ | Particle residence time [s] |

**Subscripts and Superscripts**

| | |
|---|---|
| *0* | Initial |
| *(d)a* | (Dry) Air |
| *AH* | Air Heater |
| *c* | (theoretical) cut size |
| *cr* | Critical |
| *cyc* | Cyclone |
| *db* | Dry Bran |
| *dp* | Dry Product |
| *nom* | nominal |
| *p* | Particle |
| *ref* | Reference |
| *(d)s* | (Dry) Solids |
| *salt* | Saltation |
| *t* | Terminal |
| *v* | Vapour |
| *w* | Water |
| *wb* | Wet Bran |
| *T* | Total |
| $\infty$ | Free stream |

## REFERENCES


Achaglinkame, M. A., Opoku, N., & Amagloh, F. K. (2017). Aflatoxin Contamination in Cereals and Legumes to Reconsider Usage as Complementary Food Ingredients for Ghanaian Infants: A Review. *Journal of Nutrition and Intermediary Metabolism*, **10**: 1–7. https://doi.org/10.1016/j.jnim.2017.09.001

Adegbite, S. A., Asiru, W. B., Sartas, M., Tran, T., Taborda, A. L., Chapuis, A., Ojide, M., & Abass, A. (2023). Development of a Pilot Scale Energy Efficient Flash Dryer for Cassava Flour. *Resources, Environment and Sustainability*, 100117. https://doi.org/10.1016/j.resenv.2023.100117

Banooni, S., Hajidavalloo, E., & Dorfeshan, M. (2018). A Comprehensive Review on Modelling of Pneumatic and Flash Drying. *Drying Technology*, **36**(1): 33–51. https://doi.org/10.1080/07373937.2017.1298123

Chapuis, A., Precoppe, M., Méot, J. M., Sriroth, K., & Tran, T. (2017). Pneumatic Drying of Cassava Starch: Numerical Analysis and Guidelines for the Design of Efficient Small-Scale Dryers. *Drying Technology*, **35**(4): 393–408. https://doi.org/10.1080/07373937.2016.1177537

Chiewchan, N., Mujumdar, A. S., & Devahastin, S. (2015). Application of Drying Technology to Control Aflatoxins in Foods and Feeds: A Review. *Drying Technology*, **33**(14): 1700–1707. https://doi.org/10.1080/07373937.2015.1068795

El-Behery, S. M., El-Haroun, A. A., & Abuhegazy, M. R. (2017). Prediction of Pressure Drop in Vertical Pneumatic Conveyors. *Journal of Applied Fluid Mechanics*, **10**(2): 519–527. https://doi.org/10.18869/acadpub.jafm.73.239.25384

Gomes, L. M., & Mesquita, A. L. A. (2014). *On the Prediction of Pick-Up and Saltation Velocities in Pneumatic Conveying*. **31**(01): 35–46. www.abeq.org.br/bjche

Hecht, J. P., Beimesch, W. E., Dyvelkov, K. N., Kemp, I. C., Langrish, T., Smith, F. L., & Stamper, J. A. (2019). Psychrometry, Evaporative Cooling, and Solids Drying. In D. W. Green & M. Z. Southard (Eds.), *Perry's Chemical Engineers' Handbook* (9th ed.). McGraw-Hill Education.

Incropera, F. P., DeWitt, D. P., Bergman, T. L., & Lavine, A. S. (2017). *Incropera's Principles of Heat and Mass Transfer* (Global). John & Wiley.

Kaale, L. D., Kimanya, M. E., Macha, I. J., & Mlalila, N. (2021). Aflatoxin Contamination and Recommendations to Improve its Control: A Review. *World Mycotoxin Journal*, **14**(1): 27–40. https://doi.org/10.3920/WMJ2020.2599

Kemp, I. C. (2012). Fundamentals of Energy Analysis of Dryers. In *Modern Drying Technology*, **4**: 1–45. https://doi.org/https://doi.org/10.1002/9783527631728.ch21

Klinzing, G. E. (2018). A Review of Pneumatic Conveying Status, Advances and Projections. *Powder Technology*, **333**: 78–90. https://doi.org/10.1016/J.POWTEC.2018.04.012

Knowlton, T. M., & Shrinkant, D. (2019). Gas-Solid Operations and Equipment. In Dr. D. W. Green & Dr. M. Z. Southard (Eds.), *Perry's Chemical Engineers' Handbook* (9th ed.). McGraw-Hill Education.

Kumar, P., Mahato, D. K., & Kamle, M. (2017). Aflatoxins: A Global Concern for Food Safety, Human Health and their Management. *Frontiers in Microbiology*, **7**(1): 1–10. https://doi.org/10.3389/fmicb.2016.02170

Kuye, A., Otuu, O. O., Asiru, W. B., Alenkhe, B., Sanni, L. O., Raji, A. O., Kwaya, E. I., Abdul Kareem, I. B., & Ayo, D. B. (2017). Design, Fabrication and Drying Performance of Flash Dryer for High Quality Cassava Flour. *AMA, Agricultural Mechanization in Asia, Africa and Latin America*, **48**(3): 63–70.

Mujumdar, A. (2015). Principles, Classification and Selection of Dryers. In A. S. Mujumdar (Ed.), *Handbook of Industrial Drying* (4th ed., pp. 3–29). CRC Press. https://doi.org/https://doi.org/10.1201/b17208

Munson, B. R., Gerhart, P. M., Gerhart, A. L., Hochstein, J. I., Young, D. F., & Okiishi, T. H. (Theodore H. (2018). *Munson, Young, and Okiishi's Fundamentals of Fluid Mechanics* (8th ed.). John Wiley & Sons.

Nugraha, M. G., Andersson, R., & Andersson, B. (2022). On the Sherwood number correction due to Stefan flow. *Chemical Engineering Science*, **249**: 117292. https://doi.org/10.1016/J.CES.2021.117292

Ojide, M. G., Adegbite, S., Tran, T., Taborda, L. A., Chapuis, A., Lukombo, S., Totin, E., Sartas, M., Schut, M., Becerra Lopez-Lavalle, L. A., Dufour, D., & Abass, A. (2022). Processors' Experience in the Use of Flash Dryer for Cassava-derived Products in Nigeria. *Frontiers in Sustainable Food Systems*, **5**. https://doi.org/10.3389/fsufs.2021.771639

Precoppe, M., Chapuis, A., Müller, J., & Abass, A. (2017). Tunnel Dryer and Pneumatic Dryer Performance Evaluation to Improve Small-Scale Cassava Processing in Tanzania. *Journal of Food Process Engineering*, **40**(1). https://doi.org/10.1111/jfpe.12274

Precoppe, M., Tran, T., Chapuis, A., Müller, J., & Abass, A. (2016). Improved Energy Performance of Small-Scale Pneumatic Dryers Used for Processing Cassava in Africa. *Biosystems Engineering*, **151**: 510–519. https://doi.org/https://doi.org/10.1016/j.biosystemseng.2016.10.001

Romuli, S., Abass, A., & Müller, J. (2017). Physical Properties of Cassava Grits Before and After Pneumatic Drying. *Journal of Food Process Engineering*, **40**(2). https://doi.org/10.1111/jfpe.12397

Satpati, B., Koley, C., & Datta, S. (2020). Nonlinear Model of Pneumatic Conveying Dryer for Economic Process Control. *Drying*

*Technology*, **38**(11): 1516–1537. https://doi.org/10.1080/07373937.2019.1648286

Tran, T., Abass, A., Andrade, L. A. T., Chapuis, A., Precoppe, M., Adinsi, L., Bouniol, A., Ojide, M., Adegbite, S. A., Lukombo, S. S., Sartas, M., Teeken, B., Kuate, A. F., Ndjouenkeu, R., Moreno, M., Belalcázar, J., López-Lavalle, L. A. B., & Dufour, D. (2022). Cost-Effective Cassava Processing: Case Study of Small-Scale Flash-Dryer Reengineering. In *Root, Tuber and Banana Food System Innovations* (pp. 105–143). Springer International Publishing. https://doi.org/10.1007/978-3-030-92022-7_4

Udomkun, P., Wiredu, A. N., Nagle, M., Bandyopadhyay, R., Müller, J., & Vanlauwe, B. (2017). Mycotoxins in Sub-Saharan Africa: Present Situation, Socio-Economic Impact, Awareness, and Outlook. *Food Control*, **72**(July): 110–122. https://doi.org/10.1016/j.foodcont.2016.07.039

Xiao, H. W., & Mujumdar, A. S. (2020). Importance of Drying in Support of Human Welfare. *Drying Technology*, **38**(12): 1542–1543. https://doi.org/10.1080/07373937.2019.1686476